Res Chem Intermed
DOI 10.1007/s11164-014-1579-8

Schiff base compound as a corrosion inhibitor for mild steel in 1 M HCl

Hong Liu · Lin Zhu · Qilong Zhao

Received: 2 November 2013 / Accepted: 27 February 2014

Abstract A new Schiff base compound named 4-(4′-benzoylhydrazine)-pyridinecarboxaldehyde hydrazone (BPBH) was synthesized and investigated as a corrosion inhibitor for mild steel in 1 M HCl using weight loss measurements, electrochemical techniques, and adsorption studies. The structure of BPBH was characterized by elemental analysis, infrared spectroscopy (IR), and ^{1}H nuclear magnetic resonance (NMR). The results clearly suggest that the compound acts as a mixed-type inhibitor of acid corrosion of mild steel. The adsorption of BPBH on the metal surface in 1 M HCl was found to agree with the Langmuir isotherm with a standard free energy of adsorption (ΔG^{0}_{ads}) of −31.60 kJ/mol. Scanning electron microscopy images indicate that BPBH exhibits good corrosion inhibition performance for mild steel in 1 M HCl. Quantum chemical calculations were also carried out to verify the inhibition efficiencies obtained from all the experiments.

Keywords Mild steel · Schiff base · Electrochemical technique · Quantum chemical calculations · Acid corrosion

Introduction

Acid solutions are widely used in many industrial processes, such as industrial cleaning, acid descaling, oil-well acidification, and petroleum processes, in which

H. Liu · L. Zhu (✉) · Q. Zhao
School of Chemistry and Chemical Engineering, Southwest Petroleum University, Chengdu 610500, People's Republic of China
e-mail: zhulinswpu@163.com

H. Liu
State Key Laboratory of Oil and Gas Reservoir Geology and Exploration, Southwest Petroleum University, Chengdu 610500, People's Republic of China

Published online: 14 March 2014

corrosion of equipment made from metals and alloys is regarded as a serious problem [1–6]. One of the most effective and economic approaches to protect equipment against acid corrosion is use of organic compounds as corrosion inhibitors, which is becoming increasingly popular [7–11]. Such organic compounds containing heteroatoms (oxygen, nitrogen, and sulfur) and multiple bonds exhibit excellent corrosion inhibition performance as they can easily interact with the metal surface via their adsorption behavior to assemble a protective film that can simultaneously block active sites [12–14]. It has been widely acknowledged that electron transfer from organic inhibitors to the metal occurs to form chelates on the metal surface [15]. The adsorption ability of an organic inhibitor on a metal surface depends on its physical and chemical properties and also relies on the nature and surface charge of the metal, the type of aggressive medium, and the electrochemical potential at the interface [16–18].

Due to their great flexibility and structural diversity, a wide range of Schiff bases have been synthesized and their complexation behavior studied [19, 20]. Based on the presence of nitrogen atom and the imine functional group in their structure, many Schiff bases have been reported to be effective corrosion inhibitors for various metals and alloys in acid media [21, 22]. Schiff bases can interact with metals and alloys easily to form self-assembled monolayers (SAMs). Some research works have revealed that the inhibition efficiencies of Schiff bases are much higher than those of corresponding amines and aldehydes [23]. Hydrazone compounds, one kind of Schiff base, are condensation products of a hydrazide and a ketone or aldehyde. Because of the p–π conjugation formed between the lone pair of electrons of the nitrogen atom in secondary amine, acyl group, and the double bond in imino group, hydrazone compounds are characterized by a stable structure and resistance to hydrolysis. Therefore, it is of significant and industrial importance to synthesize and investigate new hydrazone compounds as corrosion inhibitors.

In this study, a new hydrazone compound named 4-(4′-benzoylhydrazine)-pyridinecarboxaldehyde hydrazone (BPBH) was synthesized. The structure of BPBH was characterized by elemental analysis, IR, and ^{1}H NMR. The corrosion inhibition of the studied compound was investigated by the weight loss method and electrochemical techniques. The surface of the metal was also analyzed by scanning electron microscopy. In addition, quantum chemical calculations were carried out to explore the relationship between the molecular structure and the corrosion inhibition efficiency.

Materials and experimental techniques

Synthesis and characterization of the inhibitor

BPBH was synthesized by condensation reaction of terephthalhydrazine (4 mmol) with 4-pyridinecarboxaldehyde (4 mmol) in acetic acid (30 mL) by heating under reflux with stirring for 8 h [24–26]. The precursor compound terephthalhydrazine was synthesized according to the procedure described in the literature [27]. The

solvent was evaporated under reduced pressure, and the resulting solid was recrystallized from ethanol. The synthetic route and chemical structure of BPBH are shown in Fig. 1. Calcd. for $C_{14}H_{13}N_5O_2$: C, 59.36; H, 4.63; N, 24.72; O, 11.30. Found: C, 59.02; H, 4.51; N, 23.96; O, 11.05 %. IR (KBr, cm^{-1}): 3,238, 3,044, 1,738, 1,663, 1,541, 1,271. ^{1}H NMR (DMSO-d_6, 400 MHz, δ ppm): 12.29 (s, –CONHN=, 1H), 8.67–8.68 (m, Ar–H, 2H), 8.47 (s, CH=N, 1H), 8.05–8.12 (m, Ar–H, 4H), 7.69–7.70 (m, Ar–H, 2H), 3.90 (s, $–CONHNH_2$, 3H).

Metal specimens

Corrosion tests were performed on mild (N80) steel with composition (*w* %): C = 0.039 %, Mn = 1.57 %, Si = 0.18 %, S = 0.023 %, Mo = 0.12 %, and Cr = 0.16 %, with remainder iron.

Weight loss measurements

N80 mild steel samples (30 mm × 15 mm × 3.0 mm) were abraded with emery paper (grade 600–800–1,000–1,200) and washed with bidistilled water and acetone, then dried at room temperature (298 K). Each experiment was carried out at least three times simultaneously, and the average results were recorded.

Electrochemical measurements

Electrochemical tests (potentiodynamic polarization, electrochemical impedance spectroscopy) were carried out in a conventional three-electrode corrosion cell with platinum sheet as auxiliary electrode, saturated calomel electrode (SCE) as reference electrode, and N80 mild steel as working electrode (WE). The exposed surface area of WE was a square of size 1 cm^2. Before testing, the WE was polished with emery paper, then washed with acetone and bidistilled water. The WE was immersed in the test solution at open-circuit potential for 30 min until steady state was reached. Electrochemical measurements were carried out with an IviumStat electrochemical workstation. Electrochemical impedance spectroscopy (EIS) was carried out with an alternating-current (AC) sine wave with amplitude of 10 mV root mean square (RMS) in the frequency range from 10,000 Hz to 0.01 Hz. The potentiodynamic current–potential curves were recorded by changing the electrode potential automatically from −300 to +300 mV versus open-circuit potential at scan rate of 0.3 mV/s.

Scanning electron microscopy (SEM)

Study of the surface morphology of the metal specimens in both absence and presence of inhibitor was carried out by using a scanning electron microscope (FEI Inspect F) at accelerating voltage of 20 kV. Samples were prepared by immersing the steel samples for 2 h in 1 M HCl or 1 M HCl containing 1.0 mmol/L inhibitor. All micrographs of samples were taken at magnification of 5,000×.

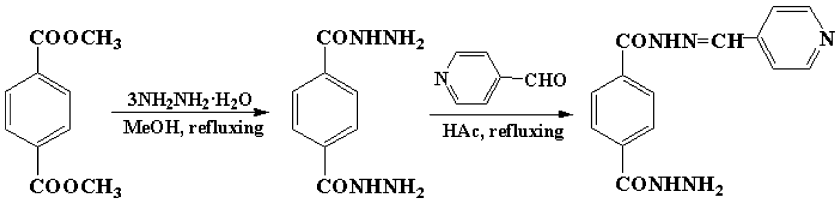

Fig. 1 Synthetic route and chemical structure of BPBH

Quantum chemical calculations

All calculations were performed at the B3LYP/6-311++G** level using the Gaussian 09W program package. The optimized molecular structure and highest occupied molecular orbital (HOMO) and lowest unoccupied molecular orbital (LUMO) surfaces were visualized using GaussView.

Results and discussion

Weight loss measurements

Effect of inhibitor concentration

Weight loss studies were performed in the absence and presence of different concentrations of BPBH by immersion for 2 h at room temperature. The corrosion rate (CR, mg/cm^2 h) was calculated as

$$\text{Corrosion rate (CR)} = \frac{W}{At}, \tag{1}$$

the percentage inhibition efficiency (η) was calculated as

$$\eta(\%) = \frac{W_0 - W}{W_0} \times 100, \tag{2}$$

and the degree of surface coverage (θ) was calculated as

$$\theta = \frac{W_0 - W}{W_0}, \tag{3}$$

where W_0 and W are the weight losses of N80 mild steel with and without inhibitor, respectively, and A and t stand for the total corroding area and the immersion period, respectively. The weight losses of the steel samples were obtained from different experiments upon addition of different concentrations (0.05–1.0 mmol/L) of BPBH, as listed in Table 1. It is conspicuous that the inhibition efficiency increases and the corrosion rate decreases with increasing inhibitor concentration (Fig. 2). The inhibition efficiencies of BPBH obtained from the weight loss measurements are in reasonably good agreement with those extracted from the electrochemical methods below.

Table 1 Corrosion parameters obtained from weight loss measurements for N80 steel in 1 M HCl in presence of different concentrations of BPBH at 298 K

Inhibitor concentration (mmol/L)	Weight loss (mg/cm^2)	η (%)	θ	CR (mg/cm^2 h)
Blank	0.0154	–	–	0.65
0.05	0.0122	21.4	0.214	0.51
0.1	0.0086	44.6	0.446	0.36
0.5	0.0027	82.6	0.826	0.11
0.8	0.0015	90.3	0.903	0.06
1.0	0.0010	93.6	0.936	0.04

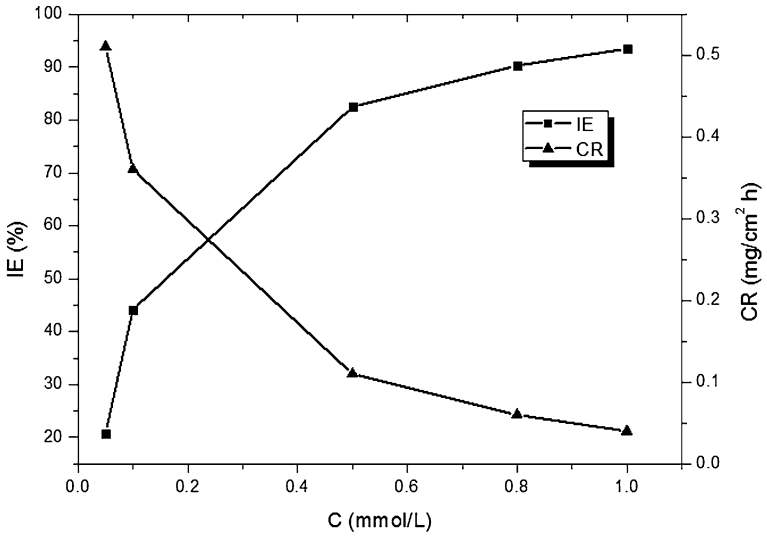

Fig. 2 Variation of inhibition efficiency (IE) and corrosion rate (CR) in 1 M HCl versus BPBH concentration

Effect of temperature

To explore the relationship between the inhibition efficiency of the studied compound and temperature, several experiments were carried out on the inhibition performance of the optimum concentration (1.0 mmol/L) of BPBH for N80 steel in 1 M HCl at temperatures ranging from 298 to 328 K. The immersion time of the weight loss measurements was 2 h. The results are shown in Fig. 3, clearly showing that the inhibition efficiency gradually decreased with increasing temperature.

Effect of immersion time

Figure 4 shows the relationship between the stability of the adsorbed inhibitor film in mild steel/acid solution and the immersion time ranging from 2 to 24 h (2, 4, 6,

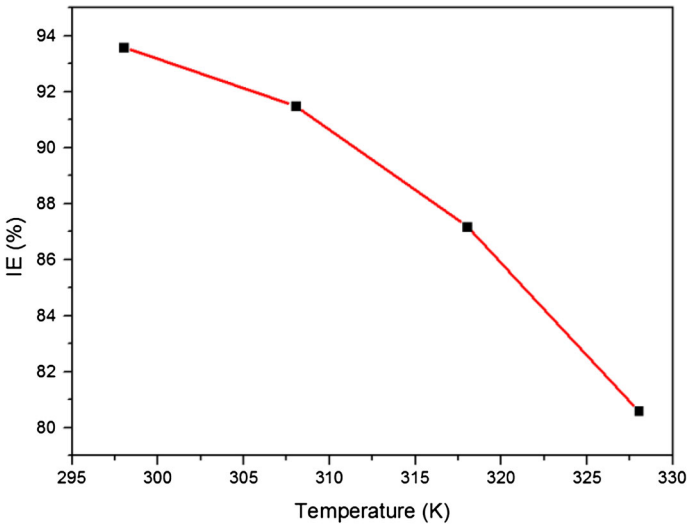

Fig. 3 Variation of inhibition efficiency versus temperature of the solution for N80 steel in presence of BPBH (1.0 mmol/L)

12, and 24 h) with 1.0 mmol/L inhibitor at room temperature. As shown in Fig. 4, it was found that the inhibition efficiency increased slightly from 93.6 to 95 % during 2–12 h in 1 M HCl, which can be explained by the formation of a protective film on the mild steel surface with increasing time [28]. However, the inhibition efficiency gradually decreased to 87 % during 12–24 h due to decreasing adsorption and increasing desorption [22, 29].

Polarization measurements

The potentiodynamic polarization curves of N80 mild steel in 1 M HCl in the absence and presence of different concentrations of inhibitor are shown in Fig. 5. Table 2 presents the electrochemical corrosion kinetic parameters, i.e., the corrosion potential (E_{corr}), the cathodic and anodic slopes (β_c, β_a), and the corrosion current density (i_{corr}). The inhibition efficiency was calculated from the measured i_{corr} values using the following equation:

$$\eta\,(\%) = \frac{(i^0_{corr} - i_{corr})}{i^0_{corr}} \times 100, \tag{4}$$

where i^0_{corr} and i_{corr} are the corrosion current density of mild steel without and with inhibitor, respectively. Table 2 reveals that the inhibition efficiency increased and i_{corr} decreased as the inhibitor concentration was increased, as the adsorption process taking place on the metal surface gradually strengthened with increasing inhibitor concentration. The values of β_c changed slightly on addition of BPBH, suggesting that the cathodic process was activation controlled, whereas addition of

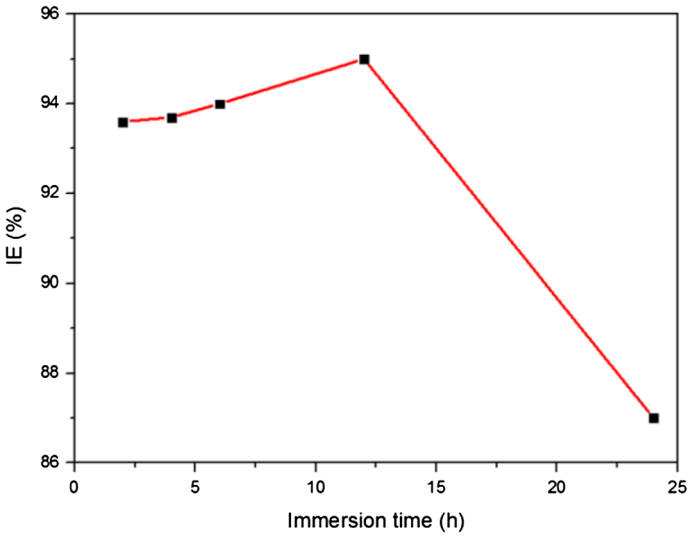

Fig. 4 Variation of inhibition efficiency versus immersion time for N80 steel in presence of BPBH (1.0 mmol/L)

BPBH did not modify the mechanism of the hydrogen evolution process. The shift of β_a may be due to adsorption of inhibitor molecules on the metal surface. The inhibition efficiency reached 85.9 % at the optimal concentration (1.0 mmol/L) of BPBH, so we can conclude that BPBH is an efficient corrosion inhibitor for mild steel in HCl solution [30]. Decreases in both the cathodic and anodic currents are noted in Fig. 5. Simultaneously, the change in the E_{corr} value calculated from Table 2 is smaller than 85 mV. The above facts confirm that BPBH can be regarded as a mixed-type inhibitor [31].

Electrochemical impedance measurements

Figure 6 shows the Nyquist plane plots for N80 steel in 1 M HCl in the absence and presence of various concentrations of inhibitor at room temperature. The impedance diagrams obtained have the appearance of a semicircle in all experiments, indicating that a charge-transfer process mainly controls the corrosion of mild steel and a protective film is formed on the metal surface. The Nyquist diagrams in Fig. 6 are not perfect semicircles as a result of the roughness and other inhomogeneities of the metal surface. Generally, the shape of impedance diagrams can be used to deduce kinetic information regarding the electrode interface between the metal and acid solution [32]. The electrochemical corrosion kinetic parameters of the studied compound are listed in Table 3. R_s is solution resistance. The inhibition efficiency was calculated from the following equation:

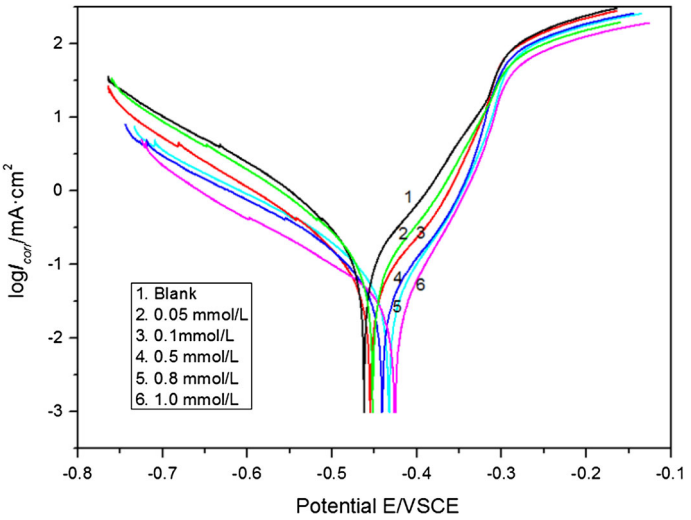

Fig. 5 Potentiodynamic polarization curves for N80 steel in 1 M hydrochloric acid in the absence and presence of different concentrations of BPBH at 298 K

Table 2 Electrochemical data for N80 steel with different concentrations of BPBH at 298 K

Inhibitor concentration (mmol/L)	E_{corr} (V/SCE)	i_{corr} (μA/cm^2)	β_a (V/dec)	β_c (V/dec)	η (%)
Blank	−0.4621	157	0.214	0.234	–
0.05	−0.4521	106	0.212	0.227	32.3
0.1	−0.4551	64	0.193	0.225	59.2
0.5	−0.4416	51	0.217	0.223	67.5
0.8	−0.4326	31	0.226	0.213	80.3
1.0	−0.4269	22	0.224	0.221	85.9

$$\eta\,(\%) = \frac{(R_{ct} - R'_{ct})}{R_{ct}} \times 100, \tag{5}$$

where R'_{ct} and R_{ct} are the values of the charge-transfer resistance observed in the absence and presence of inhibitor, respectively.

As can be seen from Fig. 6, the size of the depressed semicircle increased with increasing inhibitor concentration, reaching a maximal value for inhibitor concentration of 1.0 mmol/L. The corresponding Bode plots are shown in Fig. 7, and the best-fit electrical equivalent circuit for the systems is shown in Fig. 8. The impedance of the constant-phase element (CPE) is given by the following equation:

$$Z_{CPE} = Q^{-1}(j\omega)^{-n}, \tag{6}$$

where Q is the magnitude of the CPE, j is the imaginary unit, ω is the angular frequency ($\omega = 2\pi f$, where f is the frequency in Hz), and n is the phase shift, which

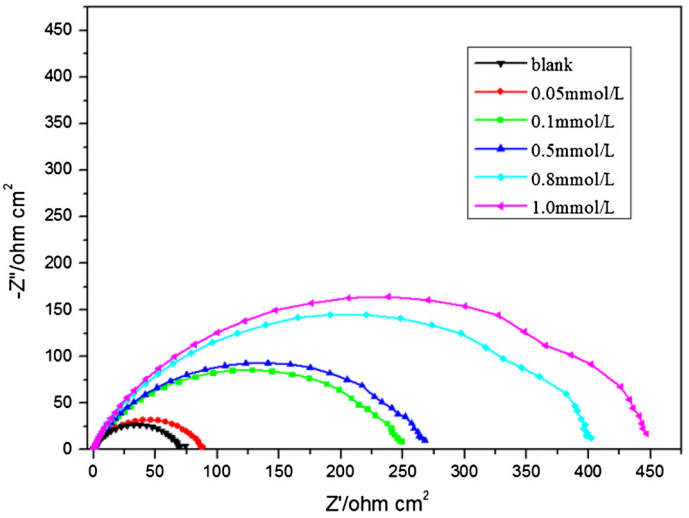

Fig. 6 Nyquist plots of EIS measurements of N80 steel in 1 M hydrochloric acid at 298 K for different concentrations of BPBH

Table 3 Electrochemical impedance parameters obtained for N80 steel in 1 M HCl in the absence and presence of BPBH

Inhibitor concentration (mmol/L)	R_s (Ω cm^2)	R_{ct}		Q (μF/cm^2)	n	C_{dl} (μF/cm^2)	η (%)
		(Ω cm^2)	Error (%)				
Blank	0.366	70.10	2.39	242.8	0.86	123	–
0.05	0.426	89.96	2.66	241.4	0.82	105	22.1
0.1	0.527	262.1	3.69	142.5	0.82	70.5	73.2
0.5	0.476	285.2	2.96	132.0	0.82	65.3	75.4
0.8	0.460	402.9	4.44	109.0	0.83	60.6	82.6
1.0	0.556	452.9	2.40	97.0	0.83	55.7	84.5

gives details about the degree of surface inhomogeneity. When $n = 1$, this is the same equation as for the impedance of a capacitor, where $Q = C_{dl}$. In fact, when n is close to 1, the CPE resembles a capacitor, but the phase is not 90°, being constant and somewhat less than 90° at all frequencies. To obtain values for the double-layer capacitance (C_{dl}), the frequency values corresponding to the maximum imaginary component of the impedance $-Z_{max}$ were found and used in the following equation:

$$C_{dl} = Q(\omega_{max})^{n-1}, \tag{7}$$

where ω_{max} is the angular frequency at which the imaginary component of the impedance reaches a maximum.

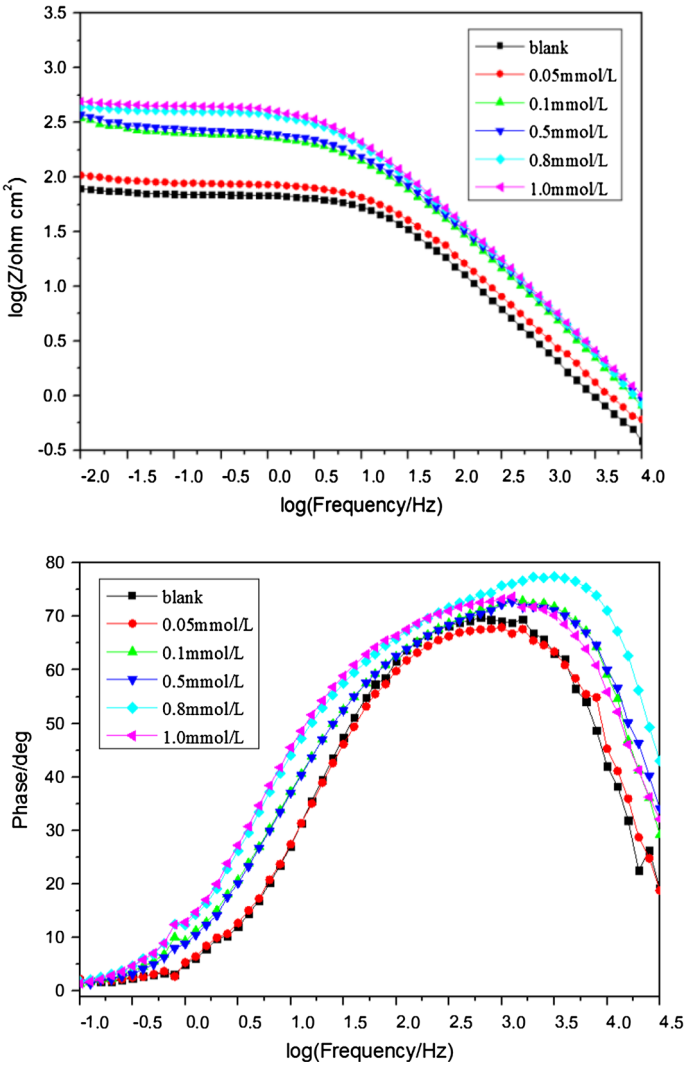

Fig. 7 Bode plots of N80 steel in 1 M hydrochloric acid in the absence and presence of BPBH

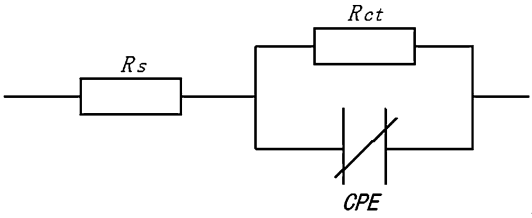

Fig. 8 Equivalent circuit for BPBH used to fit the EIS data of N80 steel in 1 M hydrochloric acid

It is clearly seen that C_{dl} decreases while the inhibition efficiency increases with increasing BPBH concentration. The decrease in C_{dl} can be attributed to a decrease in the local dielectric constant and/or an increase in the thickness of the electrical double layer, suggesting that inhibitor molecules (with low dielectric constant) displace water molecules (with high dielectric constant) originally adsorbed on the N80 steel surface. The thickness of the protective layer (d) is related to C_{dl} according to the Helmholtz model as follows:

$$C_{dl} = \frac{\varepsilon \varepsilon_0 A}{d}, \tag{8}$$

where ε is the local dielectric constant of the medium, ε_0 is the permittivity of vacuum, d is the thickness of the film, and A is the effective surface area of the electrode.

The fact that R_{ct} increases while C_{dl} decreases with increasing inhibitor concentration indicates considerable surface coverage by the inhibitor and strong bonding to the surface [33]. In the absence and in the presence of BPBH, the phase shift values remain more or less identical, indicating that a charge-transfer process controls the dissolution mechanism of N80 steel in 1 M HCl solution without and with BPBH [22].

Adsorption isotherm

To understand the mechanism of corrosion inhibition by an organic inhibitor, its adsorption behavior on the metal surface should be determined [33]. Generally, basic information on the interaction between the inhibitor and the mild steel surface can be effectively obtained through the adsorption isotherm. In this work, the results obtained by the weight loss method were used to investigate the interaction of the inhibitor with the metal surface. To obtain the isotherm, the degree of surface coverage (θ), which can be calculated from Eq. (3), must be obtained. The values of θ and inhibitor concentrations were fit to the Temkin, Frumkin, Freundlich, and Langmuir isotherms, respectively. Finally, it was found that adsorption of the synthesized compound on N80 mild steel surface in 1 M HCl obeyed the Langmuir adsorption isotherm given by the following equation:

$$\frac{C_{inh}}{\theta} = \frac{1}{K_{ads}} + C_{inh}, \tag{6}$$

where C_{inh} is the inhibitor concentration and K_{ads} is the equilibrium constant of the inhibitor adsorption process. A plot of C_{inh}/θ against C_{inh} is shown in Fig. 9. The regression coefficient is close to 1 (0.9963), so the best fit was obtained with the Langmuir adsorption isotherm, indicating that the adsorbed inhibitor molecules form a monolayer on the mild steel surface and that there is no interaction among the adsorbed inhibitor molecules [23].

The value of K_{ads} (6.248×10^3 M^{-1}) was calculated from the intercept of the fitting line. The relationship between the standard free energy of adsorption (ΔG^0_{ads}) and K_{ads} satisfies the following equation:

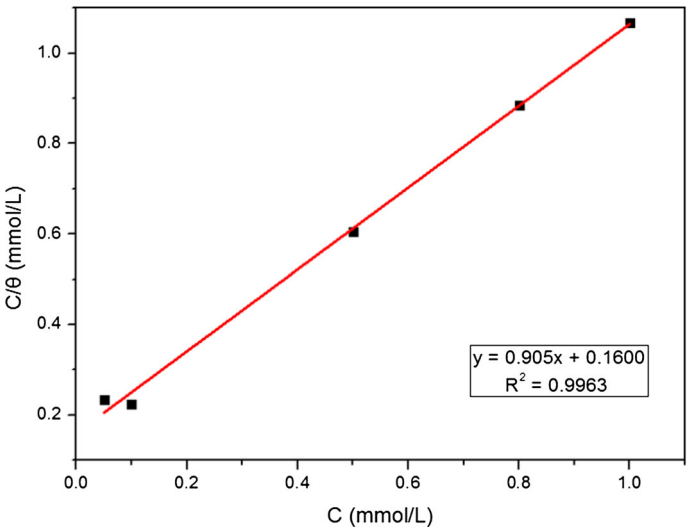

Fig. 9 Langmuir adsorption plots for N80 steel in 1 M hydrochloric acid at different concentrations of BPBH

$$K_{\text{ads}} = \frac{1}{55.5}\exp\left(-\frac{\Delta G^0_{\text{ads}}}{RT}\right), \tag{7}$$

where R is the universal gas constant, T is the thermodynamic temperature, and 55.5 is the molar concentration (mol/L) of water in the solution. In the condition studied, the calculated value of ΔG^0_{ads} was -31.60 kJ/mol. A negative value of ΔG^0_{ads} indicates stability of the adsorbed layer on the steel surface and spontaneity of the adsorption process [30]. As the value of ΔG^0_{ads} is between -20 and -40 kJ/mol, both physical and chemical adsorption were involved in the adsorption process, with chemical adsorption predominating [30, 34–36].

Scanning electron microscopy (SEM)

SEM analysis was carried out to study the changes and the effect of corrosion on the steel surface in the presence and absence of inhibitor. Figure 10a shows a polished N80 mild steel sample. Figure 10b shows a SEM image of the surface of a steel specimen immersed for 2 h in 1 M HCl, which is porous and rough; it can be deduced that the steel surface is strongly corroded in HCl. Figure 10c shows an image of the surface of a steel specimen immersed for 2 h in 1 M HCl containing 1.0 mmol/L BPBH, which is flat and smooth; this can be explained by the fact that the corrosion of the steel surface was efficiently inhibited when BPBH was present. Therefore, it can be speculated that an effective protective adsorption film was formed on the steel surface, indicating that BPBH exhibits good corrosion inhibition performance for N80 mild steel.

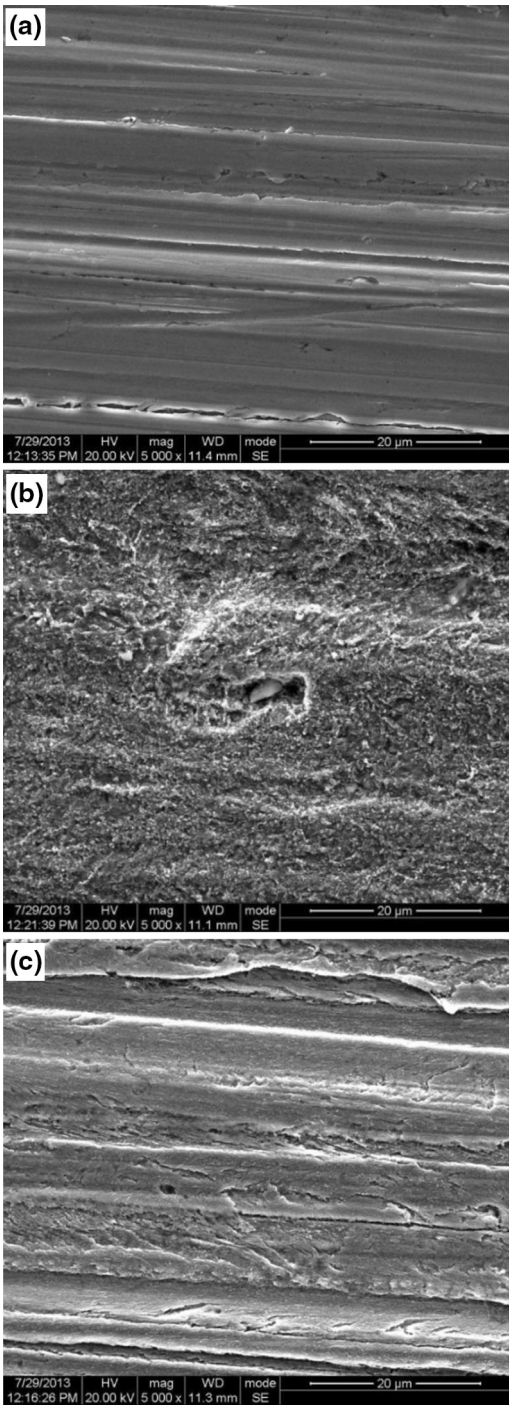

Fig. 10 SEM images of N80 steel samples: (**a**) polished surface, (**b**) after 2 h immersion in 1 M hydrochloric acid, and (**c**) after 2 h immersion in 1 M hydrochloric acid + 1.0 mmol/L BPBH

Quantum chemical calculations

To investigate the relationship between the molecular structure and the corrosion inhibition efficiency, quantum chemical calculations were undertaken [15, 37, 38]. According to frontier molecular orbital theory, only frontier molecular orbitals are involved in interactions between reactants. Hence, only the HOMO and LUMO of reactants are considered when analyzing the chelation processes of chemical adsorption [39].

Figure 11 shows the full geometry optimization of the inhibitor molecule. Figure 12a and b show the frontier molecular orbital (FMO) density distribution and energy levels of the HOMO and LUMO orbitals computed at the B3LYP/6-311++G** level for BPBH. The values of the calculated quantum chemical parameters, such as E_{HOMO} (the energy of the highest occupied molecular orbital), E_{LUMO} (the energy of the lowest unoccupied molecular orbital), ΔE ($E_{\mathrm{LUMO}} - E_{\mathrm{HOMO}}$), and μ (the dipole moment) of BPBH, are given in Table 4.

E_{HOMO} is often associated with the electron-donating ability of a molecule. Generally, the higher the E_{HOMO} value of the inhibitor, the greater its tendency to offer electrons to unoccupied *d*-orbitals of the metal, and the higher the corrosion inhibition efficiency observed for mild steel in acid solution. On the other hand, E_{LUMO} indicates the ability of the molecule to accept electrons. The lower the E_{LUMO} value of the inhibitor, the easier acceptance of electrons from the metal surface becomes. As ΔE ($E_{\mathrm{LUMO}} - E_{\mathrm{HOMO}}$) decreases, the interactions occurring on the steel surface become stronger and the efficiency of the inhibitor increases. Regarding μ, a higher value favors strong interaction of inhibitor molecules on the metal surface [28–42]. The E_{HOMO}, E_{LUMO}, ΔE, and μ values presented in Table 4 corroborate those obtained in the above experiments and show that BPBH adsorbed onto the metal surface easily. It can also be deduced that a protective layer was formed by adsorption at the mild steel/acid solution interface [28, 43].

The absolute hardness (η) and softness (δ) play an important role in measuring molecular stability and reactivity. Hard molecules have a large energy gap, whereas soft molecules have a small energy gap. Because soft molecules can easily offer electrons to an acceptor, they are more reactive than hard molecules. For the simplest transfer of electrons, adsorption can occur at the part of the molecule where the softness is highest [44]; the softness of a molecule is a local property. Generally, an inhibitor acts as a Lewis base and the metal as a Lewis acid in a corrosion system. Soft base inhibitors are most effective for acidic corrosion protection of bulk metals, which are soft acids [45]. The chemical potential (π) can measure the tendency of electrons to flow from high-potential to low-potential regions until reaching a constant state. The hardness, softness, and chemical potential are listed in Table 4. The number of electrons transferred (ΔN) was calculated from the quantum chemical method using the following equation:

$$\Delta N = \frac{(\chi_{\mathrm{Fe}} - \chi_{\mathrm{inh}})}{2(\eta_{\mathrm{Fe}} + \eta_{\mathrm{inh}})}, \tag{8}$$

where χ_{Fe} and χ_{inh} denote the absolute electronegativity of iron and the inhibitor molecule, respectively, and η_{Fe} and η_{inh} denote the absolute hardness of iron and the

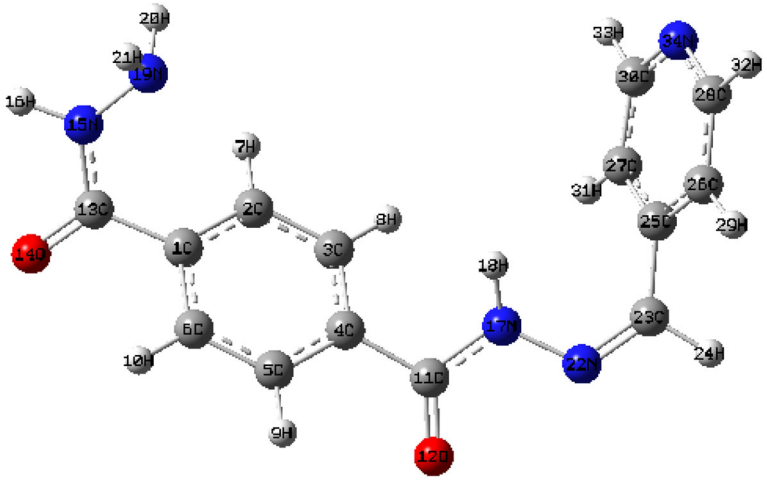

Fig. 11 Optimized structure of BPBH

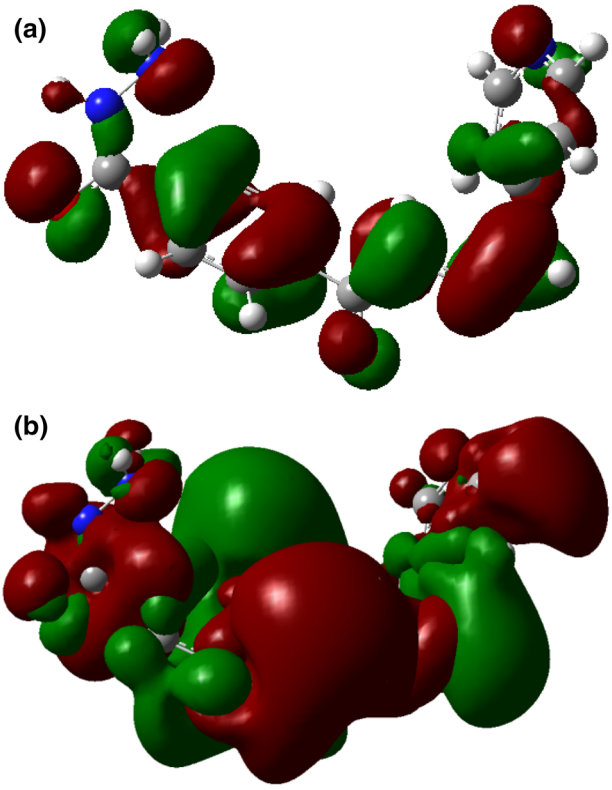

Fig. 12 Frontier molecular orbital (FMO) density distribution of BPBH: (**a**) HOMO and (**b**) LUMO

Table 4 Calculated quantum chemical parameters of BPBH

Inhibitor	E_{HOMO} (eV)	E_{LUMO} (eV)	ΔE_{L-H} (eV)	μ (Debye)	Electronegativity (eV)	Hardness (eV)	Softness (1/eV)	Chemical potential (eV)	ΔN
BPBH	−7.115	−2.462	4.653	10.864	4.789	2.327	0.430	−4.788	0.475

inhibitor molecule, respectively; a theoretical value of $\chi_{Fe} \approx 7.0$ eV was taken for iron, and $\eta_{Fe} = 0$ was taken, assuming that $I = A$ for bulk metals [46, 47].

The χ and η values of the inhibitor molecule were calculated from the following equations:

$$\chi = \frac{(I + A)}{2}; \eta = \frac{(I - A)}{2}, \tag{9}$$

where the ionization potential (I) and the electron affinity (A) are related in turn to E_{HOMO} and E_{LUMO} as follows:

$$I = -E_{HOMO}; A = -E_{LUMO}. \tag{10}$$

The softness of the inhibitor molecule is simply the inverse of the hardness: $\delta = 1/\eta$. If $\Delta N < 3.6$, the inhibition efficiency increases with increasing electron-donating ability at the metal surface [37]. In the present study, BPBH is a donor of electrons, while N80 steel surface atoms are acceptors. BPBH was bound to the N80 steel surface, and thus it formed an inhibitive adsorption layer against corrosion.

Mechanism of inhibition

The adsorption of the corrosion inhibitor at the mild steel/hydrochloric acid solution interface depends on several factors, such as the number of adsorption sites, the molecular size, and the mode of interaction with the metal surface and extent of formation of metallic complexes [48]. The adsorption process can take place through its active centers that are unshared electron pairs of heteroatoms and aromatic rings.

In acidic solutions, it is known that inhibitor molecules can be protonated as follows:

$$C_{14}H_{13}N_5O_2 + xH^+ \rightarrow [C_{14}H_{13+x}N_5O_2]^{x+} \tag{11}$$

In aqueous acidic solutions, either neutral molecules or cationic forms of BPBH molecules exist [28, 48]. It has been reported that the mechanism of corrosion inhibition for dissolution of mild steel is as follows [49]:

The anodic dissolution of iron may follow the steps:

$$Fe + Cl^- \rightarrow (FeCl^-)_{ads} \tag{12}$$

$$(FeCl^-)_{ads} \rightarrow (FeCl)_{ads} + e^- \tag{13}$$

$$(FeCl)_{ads} \rightarrow (FeCl^+)_{ads} + e^- \tag{14}$$

$$FeCl^+ \rightarrow Fe^{2+} + Cl^- \tag{15}$$

The cathodic hydrogen evolution reaction may follow the steps:

$$\mathrm{Fe} + \mathrm{H}^{+} \rightarrow (\mathrm{FeH}^{+})_{\mathrm{ads}} \tag{16}$$

$$(\mathrm{FeH}^{+})_{\mathrm{ads}} + \mathrm{e}^{-} \rightarrow (\mathrm{FeH})_{\mathrm{ads}} \tag{17}$$

$$(\mathrm{FeH})_{\mathrm{ads}} + \mathrm{H}^{+} + \mathrm{e}^{-} \rightarrow \mathrm{Fe} + \mathrm{H}_2 \tag{18}$$

It was assumed that chloride ion was first adsorbed onto the positively charged metal surface by coulombic attraction. Then, the protonated BPBH adsorbed through electrostatic interactions between the positively charged molecules and the negatively charged metal surface [50]. These adsorbed molecules interact with $(\mathrm{FeCl}^{-})_{\mathrm{ads}}$ species to form a monolayer on the surface by forming a compound. The N80 steel surface was protected from attack by aggressive chloride ions through the monomolecular layers.

Conclusions

A new hydrazone Schiff base compound BPBH was synthesized. It was found that BPBH shows good inhibition efficiency for N80 mild steel in 1 M HCl. The inhibition efficiency of BPBH increases with increasing inhibitor concentration and decreases with higher temperature and longer exposure period. The polarization curves imply that BPBH acts as a mixed-type inhibitor. Under investigation of the steel surface, the adsorption of BPBH was found to obey the Langmuir adsorption isotherm, and its adsorption at the mild steel/hydrochloric acid interface involves both physical and chemical adsorption, with the latter being stronger.

References

1. J.I. Bregman, *Corrosion Inhibitors* (MacMillan, New York, 1963)
2. S. Ghareba, S. Omanovic, Corros. Sci. **52**, 2104–2113 (2010)
3. Z. Tao, W. He, S. Wang, S. Zhang, G. Zhou, Corros. Sci. **60**, 205–213 (2012)
4. D. Gopi, K.M. Govindaraju, L. Kavitha, J. Appl. Electrochem. **40**, 1349–1356 (2010)
5. L.J. Li, X.P. Zhang, J.L. Lei, J.X. He, S.T. Zhang, F.S. Pan, Corros. Sci. **63**, 82–90 (2012)
6. A.O. Yüce, G. Kardaş, Corros. Sci. **58**, 86–94 (2012)
7. K.C. Emregül, E. Düzgün, O. Atakol, Corros. Sci. **48**, 3243–3260 (2006)
8. A. Döner, E.A. Sahin, G. Kardas, O. Serindag, Corros. Sci. **66**, 278–284 (2013)
9. M. Bobina, A. Kellenberger, J.P. Millet, C. Muntean, N. Vaszilcsin, Corros. Sci. **69**, 389–395 (2013)
10. I. Danaee, O. Ghasemi, G.R. Rashed, M. RashvandAvei, M.H. Maddahy, J. Mol. Struct. **1035**, 247–259 (2013)
11. A.S. Patel, V.A. Panchal, G.V. Mudaliar, N.K. Shah, J. Saudi, Chem. Soci. **17**, 53–59 (2013)
12. S.S. Abd-El-Rehim, M.A.M. Ibrahim, K.F. Khalid, J. Appl. Electrochem. **29**, 593–599 (2002)
13. S. Rengamani, S. Muralidharan, M. AnbuKulamdainathan, I.S. Venkatakrishna, J. Appl. Electrochem. **24**, 355–359 (1994)
14. M. Ajmal, A.S. Mideen, M.A. Quraishi, Corros. Sci. **36**, 79–84 (1994)
15. H. Ju, Z.P. Kai, Y. Li, Corros. Sci. **50**, 865–871 (2008)
16. I. Ahamad, M. Quraishi, Corros. Sci. **51**, 2006–2013 (2009)
17. I. Ahamad, M. Quraishi, Corros. Sci. **52**, 651–656 (2010)
18. S.K. Shukla, M. Quraishi, Corros. Sci. **52**, 314–321 (2010)

19. A.D. Azazl, S. Celen, H. Namlil, O. Turhanl, Proc. Ind. Acad. Sci. **32**, 884–888 (2007)
20. H.D. Yin, H. Liu, M. Hong, J. Organomet. Chem. **713**, 11–19 (2012)
21. I. Ahamad, R. Prasad, M.A. Quraishi, Corros. Sci. **52**, 933–942 (2010)
22. I. Ahamad, C. Gupta, R. Prasad, M.A. Quraishi, J. Appl. Electrochem. **40**, 2171–2183 (2010)
23. P. Pelagatti, M. Carcelli, F. Franchi, C. Pelizzi, A. Bacchi, A. Fochi, H.-W. Frühauf, K. Goubitz, K. Vrieze, Eur. J. Inorg. Chem. **3**, 463–475 (2000)
24. H. Meng, Z.F. Xie, J. Hu, F.M. Liu, Chin. J. Org. Chem. **28**, 1423–1427 (2008)
25. D.Q. Long, S.S. Chen, D.J. Li, J. JiangXi Normal Univ. Nat. Sci. **30**, 372–374 (2006)
26. X.H. Sun, Y. Tao, Y.F. Liu, B. Chen, Acta Chim. Sin. **66**, 234–238 (2008)
27. D.Q. Long, S.S. Chen, H. Chen, Chin. J. Synth. Chem. **14**, 069–071 (2006)
28. A. Singh, J.N. Avyaya, E.E. Ebenso, M.A. Quraishi, Res. Chem. Intermed. **39**, 537–551 (2013)
29. D.F. Shriver, P.W. Atkins, C.H. Langford, *Inorganic Chemistry*, 2nd edn. (Oxford University Press, Oxford, 1994)
30. S. Şafak, B. Duran, A. Yurt, G. Türkoğlu, Corros. Sci. **54**, 251–259 (2012)
31. Y. Abboud, B. Hammouti, A. Abourriche, A. Bennamara, H. Hannache, Res. Chem. Intermed. **38**, 1591–1607 (2012)
32. W.J. Lorenz, F. Mansfeld, Corros. Sci. **21**, 647–672 (1981)
33. M.A. Quraishi, D. Jamal, Mater. Chem. Phys. **68**, 283–287 (2001)
34. E.A. Noor, Int. J. Electrochem. Sci. **2**, 996–1017 (2007)
35. M. Bhupendra, S.J. Mistry, Res. Chem. Intermed. **39**, 1049–1068 (2013)
36. S. John, K.M. Ali, A. Joseph, Bull. Mater. Sci. **34**, 1245–1256 (2011)
37. I. Lukovits, E. Kalman, F. Zucchi, Corrosion **57**, 3–8 (2001)
38. I. Ahamada, R. Prasadb, M.A. Quraishia, Mater. Chem. Phys. **124**, 1155–1165 (2010)
39. J. Fang, J. Li, J. Mol. Struct. Theochem. **593**, 179–185 (2002)
40. G. Gece, Corros. Sci. **50**, 2981–2992 (2008)
41. R.M. Issa, M.K. Awad, F.M. Atlam, Appl. Surf. Sci. **255**, 2433–2441 (2008)
42. B.D. Mert, M.E. Mert, G. Kardas, B. Yazici, Corros. Sci. **53**, 4265–4272 (2011)
43. N. Missoum, A. Guendouz, N. Boussalah, B. Hammouti, A. Chetouani, M. Taleb, A. Aouniti, S. Ghalem, Res. Chem. Intermed. **39**, 3441–3461 (2013)
44. S. Martinez, Mater. Chem. Phys. **77**, 97–102 (2002)
45. L.F. Mar, O.O. Xometl, M.A.D. Aguilar, E.A. Flores, P.A. Lozada, F.J. Cruz, Corros. Sci. **61**, 171–184 (2012)
46. J.C. Slater, *Introduction to Chemical Physics* (Dover, New York, 1970)
47. M.J.S. Dewar, W. Thiel, J. Am. Chem. Soc. **99**, 4899–4907 (1977)
48. I. Ahamad, R. Prasad, E.E. Ebenso, M.A. Quraishi, Int. J. Electrochem. Sci. **7**, 3436–3452 (2012)
49. W. Li, Q. He, C. Pei, B. Hou, Electrochim. Acta **52**, 6386–6394 (2007)
50. M.A. Quraishi, M.Z.A. Rafiquee, S. Khan, N. Saxena, J. Appl. Electrochem. **37**, 1153 (2007)